

# Chapter 6

## Evaluation of a regional climate model

### 6.1 Motivation

Although precipitation is one of the key parameters of the hydrological cycle it is still not adequately represented in climate models. The reason for that lies mainly in the sub-grid character of precipitation processes. Most convective processes, such as thunderstorms, occur in scales smaller than the relatively coarse grid size of climate models. A necessary statistical approximation generates precipitation uniformly in each grid box, and therefore can not simulate the actual spatial patterns and rain intensity peaks.

The complexity of the interactions of precipitation with other components of the model system raises questions of considerable interest for a better understanding of the inlaying processes. Precipitation is, in fact, a function of almost every physical process within the model. That is resulting in a high sensitivity of the precipitation field on inaccurate simulations of other components, such as clouds, surface heating or the representation of fronts. Erroneous simulation of solar heating at the surface, for example, will show up in the precipitation field and furthermore affect evaporation, soil moisture or temperature distribution. Hence, evaluation of precipitation is not only important to evaluate the parameter "precipitation" itself, but also a good diagnostic tool (*'test bed'*) for the overall performance of a climate model. Albeit validation of total precipitation amounts in large time-scales (e.g. yearly or monthly sums) exhibit in general reliable results compared to observations, the representation of the diurnal cycle is inaccurate in the bulk of climate models in which it occurs at the hour of strongest heating. That is up to three hours too early. (Trenberth et al., 2003).

The atmosphere exhibits strong diurnal variations in a number of parameters, such as surface temperature, cloudiness or precipitation due to daily cycle of solar irradiance. This kind of variability are often referred as to the *atmospheric tides*. I would like to refer to documentations about the diurnal variability of atmospheric parameters, such as cloud cover (Morcrette, 1991) or precipitation (Dai et al., 1999). The majority of the studies is focused

on the diurnal cycle in a global observations or on the diurnal cycle in the tropics (Dai, 2001; Betts and Jakob, 2002; Nesbitt and Zipser, 2003).

As described before, precipitation in cyclonic-dominated mid-latitudes can generally separated in different modi as an expression of the initial source: frontal and convective. Frontal systems have special structure in 2D-horizontal precipitation maps. They are usually identified by a longish shape with an extension of several hundred kilometres and moderate and homogeneously distributed rain rates. In the previous chapters of the here presented work I introduced a new automatic algorithm based on textural and region-based shape analysis to separate frontal precipitation in BALTRAD radar composites. The frontal fraction was estimated to two third of the overall precipitation in the Baltic area for the period of 2000 to 2002. While frontal precipitation is usually assumed as free of diurnal preferences, convective shifting of air is directly related to the heating of the underlying surface and exhibits therefore a strong diurnal cycle. For the purpose of this section - the evaluation of the diurnal cycle of a regional climate model - it seems worthwhile to distinguish precipitation into these two partitions. An examination of the convective partition allows us to evaluate more thoroughly the special problems of atmospheric tides. The assumption, that frontal precipitation has no diurnal variability, is certainly true for the frequency of the number of frontal overpasses, however Tetzlaff and Hagemann (1986) presumed, that the frequency of rain decreases also in frontal systems in afternoon in summer due to instable atmospheric layering in pre-frontal regions.

To my knowledge, there have not been any studies of the diurnal cycle of precipitation according to its type of source by a larger data set than synoptic data of one local point. The possibilities to investigate the diurnal cycle of precipitation are rare. The bulk of synoptical stations provide point measurements only on a twice-daily basis. Once one have sufficient temporal highly resolved gauge measurements the areal information can be achieved by interpolation (e.g “kriging”) techniques. Satellite methods with matching techniques of microwave, visible and infrared sensors exhibit hopeful approaches, but still lack at rain in stratiform areas. Currently, the best suited instrument is the ground-based radar. It’s advantages are the high temporal sample density and a reliable rain/no-rain detection. Quantitative estimation of precipitation is, especially if one tries to accumulate over a long time span, such as a month, insufficient. In order to cover large areas, such as the Baltic catchment, a radar composite product is required.

The evaluation of the climate model uses the radar products of the BALTEX (*The Baltic Sea Experiment*) radar centre BALTRAD. For an additional evaluation of the overall annual sum I considered the monthly rain amounts provided by the Global Precipitation Climatology Centre (GPCC ) as well.

This chapter is organised as follows: Section 6.2 first briefly discusses the climatolog-

ical model BALTIMOS and the observational data used in this study and how they have been analysed. Section 6.3 contains results of the comparison. By the end of this chapter, conclusions are given in Section 6.4.

## 6.2 Model, observational data and analysis methods

### 6.2.1 BALTIMOS simulations

For the present study the results of the regional climate model BALTIMOS are evaluated. The model system BALTIMOS is made up of an Baltic Sea ocean model BSIOM (Lehmann, 1995), the hydrological model LARSIM (Bremicker, 2000; Richter and Ebel, 2003) and the regional atmospheric model REMO (Jacob, 2001). REMO is a three-dimensional hydrostatic atmospheric regional model. It was developed at the Max-Planck-Institut für Meteorologie (*Max-Planck-Institute for Meteorology*) in Hamburg, Germany. REMO is based on the physics of the global circulation model ECHAM-4 (Land et al., 1999). In the framework of the homonymous project BALTIMOS a fully coupled version of the model system has been developed. BALTIMOS can be used in two modes, the climate and the forecast mode. While the forecast mode simulates a consecutive time span without any assimilation routines, calculation in the climate mode are influenced by updates of the lateral boundaries every six hours. The representation of precipitation in REMO, as the uncoupled atmospheric version, was validated by Ahrens et al. (1998); Jacob (2001); Hennemuth et al. (2003); Ohmstedt et al. (2000).

The model domain comprises the full Baltic Sea drainage and adjacent parts in Central and Western Europe. REMO is set up in a 1/6 grid, which corresponds to approx. 18 x 18 km<sup>2</sup> spatial resolution in a rotated spherical grid with a pole at 170W and 32.5N. For this study REMO runs in climate mode, that means only parameters at the boundary of the domain were updated by means of ECMWF simulations each six hours. REMO has been used to study precipitation climatologies of 2000 to 2002, for which it was driven by re-analyses from ECMWF at the lateral boundaries. More detailed information about the model can be obtained by Jacob (2001).

Simulation output of precipitation includes the separation between a small-scale and a large-scale partition. Small-scale precipitation are associated with convective precipitation through cumulus generation and is regulated by the Tiedke scheme (Tiedke, 1989), while the large-scale part is determined by prognostic treatment. Humidity fluxes, as evaporation or advection into or out of a grid box are considered in the model.

Jacob (2001) compared the REMO output with the data of the BALTEX Hydrological data centre, which is mainly based on synoptical observations. Hennemuth et al. (2003)

focused on the comparison with two climate models and an interpolated field from observations by ships to investigate precipitation exclusively above the water body of Baltic Sea area. Both publications found a high agreement in respect of monthly and annual amounts and variability.

### **6.2.2 Observational data**

For comparison with BALTIMOS simulations, two observational data sets of precipitation are used, the rainfall data of the Global Precipitation Climatology Centre, referred as to GPCC, and radar data of the BALTEX radar data centre BALTRAD.

GPCC data are derived from quality-controlled rain gauge measurements and collected by the German Weather service DWD. The data comes on a monthly basis on two different resolutions of a  $2.5^\circ$  and a  $1^\circ$  longitude/latitude grid derived by an spatial interpolation procedure. All rain gages within a box are sampled and averaged for the rain amount value for this grid box. There are no ship measurements or any other ocean observations included. For this study only grid boxes with at least one rain gauge within were used. More information about GPCC data set can be found in an article by Rudolf and Schneider (2004).

Radar-based precipitation data set BALTRAD data set has already introduced in Section 2.2 on page 10.

### **6.2.3 Methods of comparison**

The comparison of simulated data of BALTIMOS with BALTRAD was done by reducing the resolution of radar observations from 2 kilometres to coarse model resolution of 18 kilometres by simple averaging the rain rates over all radar observations within a BALTIMOS grid box and temporal averaging of all quarterly per hour to hourly values. Subsequently, the frontal/convective algorithm (see Chapter 3) was applied to determine the frontal fraction on overall precipitation. As described before, the classification tool is based on a artificial neural network. This was originally trained for a resolution of 2 kilometres spatial resolution. Thus, it had to be re-trained for the spatial resolution of the BALTIMOS grid (grid size 18 kilometres). Since the general classification scheme is based on textural information it is assumed that the coarser spatial resolution of BALTIMOS decreases the performance. However, a visual check of the classification performance for a row of identical scenes in 2 kilometres resolution to the 18 kilometres resolution scheme has shown a good agreement. The separation of rain into frontal and convective partition can be regarded as a classification into a part without diurnal preferences (frontal partition) and one with considerable diurnal variability (convective partition).

Overall diurnal variability studies are examined with initial separation in different classes of precipitation (frontal or convective) as well as in the type of surface (land or sea). The mean diurnal anomaly of precipitation for each grid box is subjected to a simple harmonic Fourier analysis as described in Chapter 5 (Page 10). This enables seeing regional particularities by displaying the spatial distribution of diurnal cycle parameters in geographical maps.

## 6.3 Results

### 6.3.1 General features

The studies of Jacob (2001) and Hennemuth et al. (2003) have already compared precipitation in the atmospheric module of BALTIMOS with observations. Their results show fair agreement between the monthly means of simulations and observations. Nevertheless, the performance of BALTIMOS on the overall precipitation as well as their spatial patterns is evaluated again in this section to provide a further evidence of the reliability of simulation results of BALTIMOS.

Fig. 6.1 shows the spatial distribution of yearly precipitation amounts for the period 2000 to 2002 for BALTIMOS and GPCC data. Since GPCC represents gauge measurements, this comparison is limited to land surface simulations. The model is able to reproduce the broad spatial patterns observed by the precipitation gauges, such as maximum rain sums west of the Norwegian mountain chain and the Alpes as well as areas with low rain rates in southeast Central Europe and northeast Scandinavia. Considerable differences occur in eastern part of the model domain (e.g. Belarus), where the model has much higher values than the observations. However, some discrepancy may partly stem from the low observation density in the southern part of this region, especially on higher altitudes in the Carpathian Mountains. Furthermore, there is an overestimation of up to 200 mm in the yearly rain amount in parts of Norway and Sweden. Features of some special periods are well captured, such as the regions with low rain rates in 2000 in Southern Europe and in 2002 in northern parts of Baltic Sea and adjoined land regions. However, BALTIMOS overestimates the total precipitation up to 30 % comparing with GPCC as shown in Table 6.1. In summary, BALTIMOS tends to produce more rain amount in comparison with gauge measurements.

Fig. 6.2 examines the frequency of occurrence statistics of rain rates in simulations and observations. The left panel shows the cumulative percentage of pixels versus the rain rate. The point of the graphs intersection with the y-axis gives the rain-free fraction. While the radar observations exhibit more than 82 percent rain-free pixels, this value is in BALTIMOS only 59 percent, so that BALTIMOS has more than twice of rain pixels (41 percent in

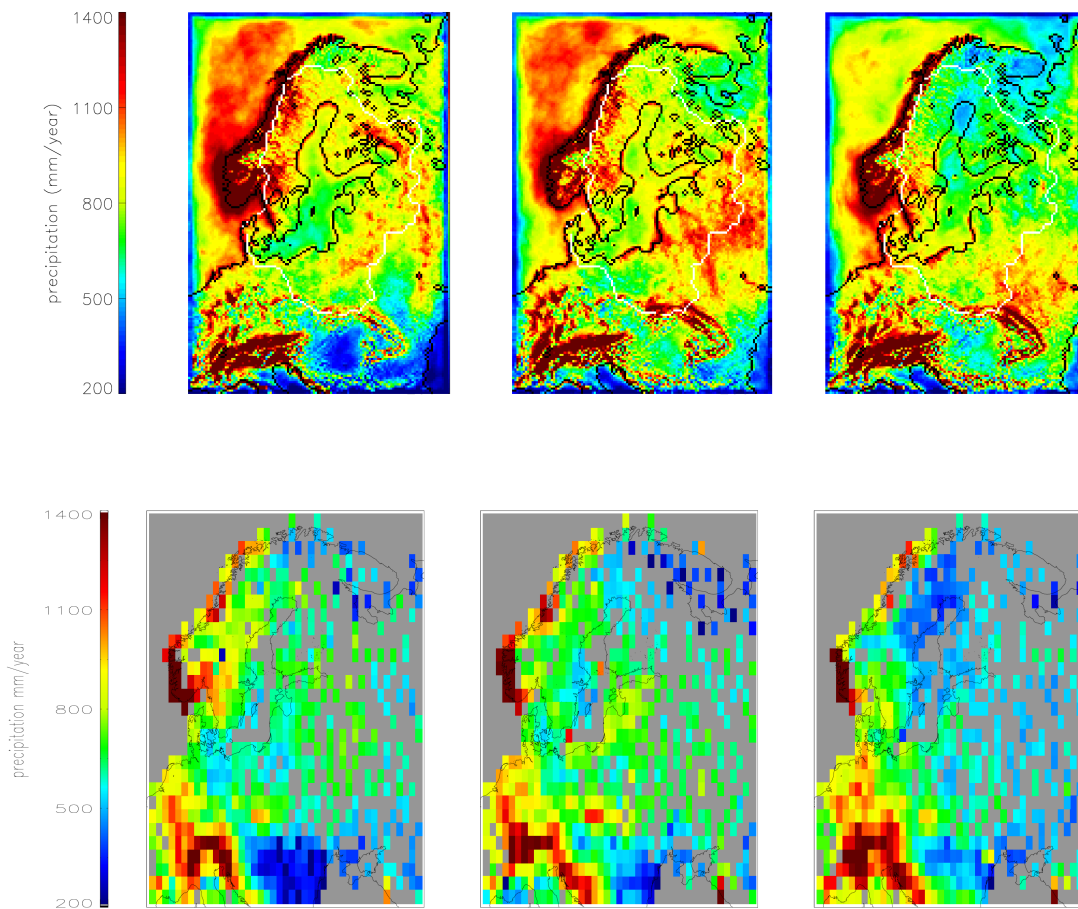


**Figure 6.1:** Annual precipitation sums of 2000-2002 simulated by BALTIMOS (upper panels) and from GPCCC observations (lower panels).

BALTIMOS to 18 percent in BALTRAD). While the highest values in the simulations reach approx. 5 mm/h there are observations of more than 20 mm/h (not shown in Fig. 6.2). The peak value is, in fact, even higher in the original high-resolution data set without the reducing to BALTIMOS grid.

The middle panel of Fig. 6.2 illustrates the cumulative percentage of total rain amount in mm/h expressed as the fraction of all rain pixels. To give an example, in BALTIMOS approx. 75 percent of the total amount is provided by rain events lower than 1 mm/h intensity (intersection of the graph with the 1mm/h-parallel to y-axis). In contrast, this amount is well below at 60 percent in observations. In general, a bigger fraction of the rain amount in BALTIMOS are contributed by weak rain intensities.

The frequency of occurrence of weak precipitation events with rain rates of less than 1 mm/h are considerably higher in simulations than in observations (right panel of Fig. 6.2). The highest number of rain pixels in BALTIMOS is at rain rates at about 0.04 mm/h and in

**Table 6.1:** Annual precipitation sum for all surface types ( $P_{all}$ ) as well as divided in land ( $P_l$ ) and sea ( $P_s$ ) in mm for BALTIMOS simulations and BALTRAD and GPCC observations.

Year	BALTIMOS			BALTRAD			GPCC
	$P_{all}$	$P_l$	$P_s$	$P_{all}$	$P_l$	$P_s$	$P_l$
2000	879	901	801	573	609	486	684
2001	907	918	868	830	882	701	670
2002	783	788	768	749	787	663	584

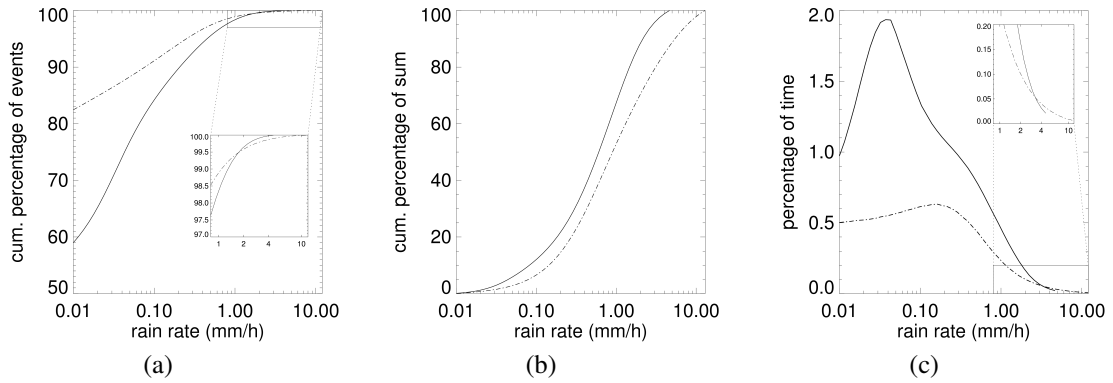


**Figure 6.2:** Distribution of frequency of occurrence of precipitation intensity in BALTRAD (dashed lines) and BALTIMOS (solid lines). Left panel shows the cumulative percentage of rain events versus logarithmic stretched rain rate with a inset for rain rates beginning at 1mm/h. Middle panel shows the cumulative fraction on precipitation sum. Right panel shows the normalised frequency of occurrence of rain intensity with a inset for rain rates beginning at 1mm/h. The x-axes are respectively divided in 51 bin ranges in the logarithmic space from 0.01 mm/h to 15 mm/h in the form  $b_i = [b_i, b_{i+1}]$  according to  $b_i = \exp\left(\log(0.01) + i \cdot \left(\frac{\log(15) - \log(0.01)}{51}\right)\right)$  with  $b_i$  in unit mm/h.

BALTRAD at 0.2 mm/h. Note, that in all three panels of Fig. 6.2 logarithmic scaling equals the bin size of the x-axis.

The upper two panels of Figs. 6.3, 6.4 and 6.5, show respectively time series of daily values of the frequency of occurrence of rain and the rain amount averaged over all co-located pixels. The day-to-day variability is well captured. However, the frequency of rain events are always bigger in the simulations than in observations. In periods with high daily rain amounts, such as at days nr. 190-260 in 2001 or around day nr. 180 in 2002, BALTIMOS underestimates considerably the rain sum. This is accompanied by higher rain intensities in observations.

In summary of this section, BALTIMOS tends to produce more precipitation amount in comparison to observations mainly due to a heightened number of weak precipitation events.

### 6.3.2 Frontal fraction

**Table 6.2:** Annual frontal fraction for all surface type ( $F_{all}$ ) and divided in land ( $F_l$ ) and sea ( $F_s$ ) in percent for BALTIMOS simulations and BALTRAD observations.

Year	BALTIMOS			BALTRAD		
	$F_{all}$	$F_l$	$F_s$	$F_{all}$	$F_l$	$F_s$
2000	0.60	0.60	0.60	0.55	0.53	0.63
2001	0.58	0.57	0.59	0.56	0.53	0.62
2002	0.52	0.52	0.53	0.57	0.55	0.61

Table 6.2 compares frontal fraction determined by simulations and observations for all co-located grid points. The overall frontal fraction in observations lies at about 56 percent. There is no interannual variability. The partition on frontal precipitation is about 10 percentage points higher than that above land surface.

While the annual results of frontal fraction differ by only a few percentage points and are in a good agreement to the observations (Table 6.2), the inter-annual differences between BALTIMOS and BALTRAD are considerably high (lower panels in Figs. 6.3, 6.4 and 6.5). The patterns of all three years resemble each other: The frontal fraction is higher in cold season than in summer in observations as well as in BALTIMOS. However, there is an over-estimation of frontal fraction in simulations from October to about April. The discrepancy may be explained by the following mechanism: Since BALTIMOS produces too many weak rain pixels, it is in general more likely that the size of contiguous rain regions exceed the size of area threshold for the preliminary distinction of the possibility of frontal precipitation. In addition, in periods of high frontal activity it is more likely that frontal systems include



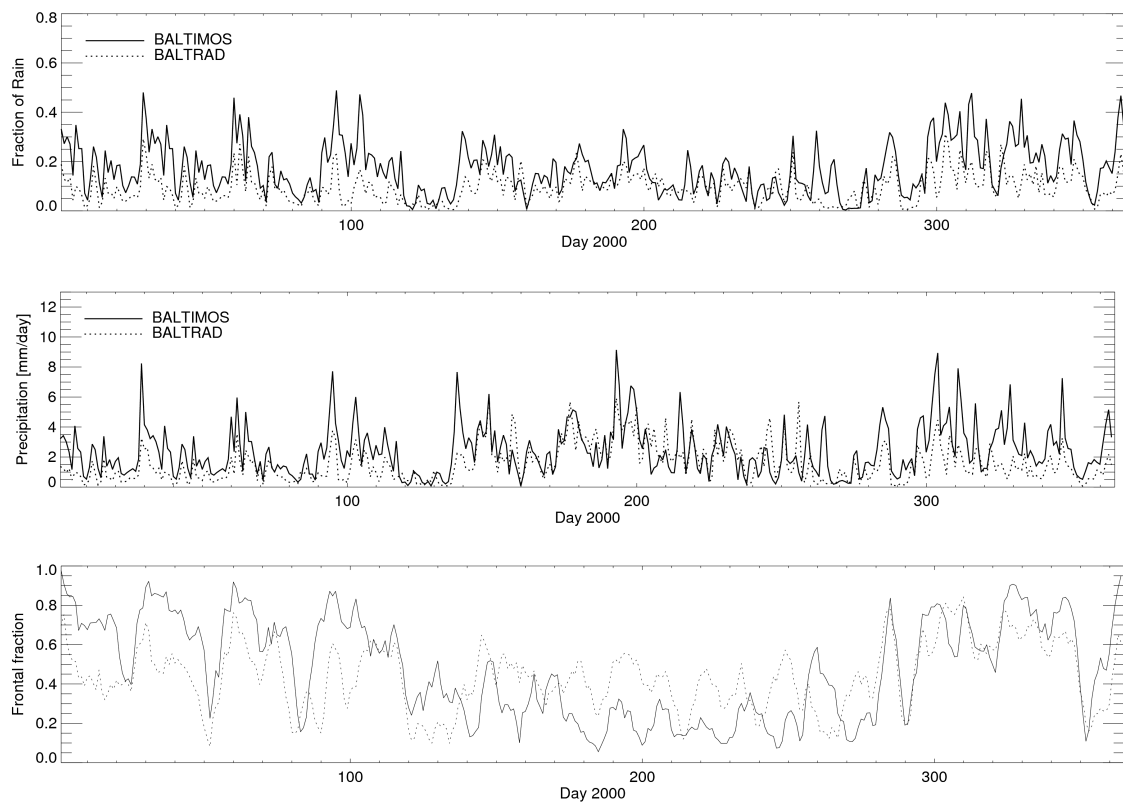


**Figure 6.3:** Daily precipitation simulated by BALTIMOS (solid lines) and in BALTRAD radar observations (dashed lines) for 2000. The upper panel shows the fraction of rain pixels with values below 0.2 mm/h on overall pixels. The middle panel shows the corresponding average daily sums for the Baltic area. The lower panel shows the fraction of frontal precipitation events on all precipitation events as a 5-day average.

smaller areas if the number of rain pixels is high. These areas may be classified as convective if they are not spatially connected to larger rain areas in the observation data set.

In warm season (from April to September) the model underestimates the frontal fraction. This is mostly the case in 2002 (Fig. 6.5). The more daily rain amount the more the frontal fraction are underestimated. The fraction of rain events does not increase at these time periods. The conclusion is, that periods with high rain intensities are likely for a underestimation of frontal fraction. the reason for that is not clear at the moment and needs further investigations. Nethertheless, beside the direct comparison of daily frontal fraction, it appears that the day-to-day variability is well captured. The recognition of frontal overpasses works.

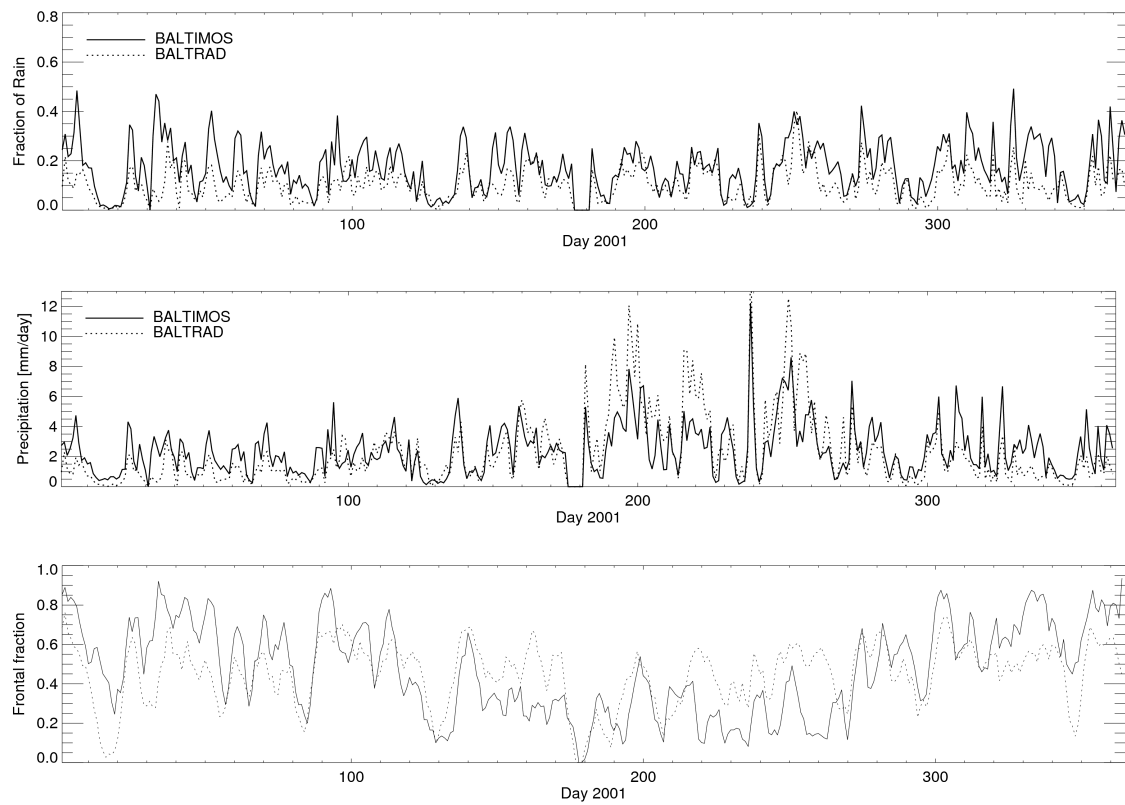


**Figure 6.4:** Same as Fig. 6.3, but for 2001.

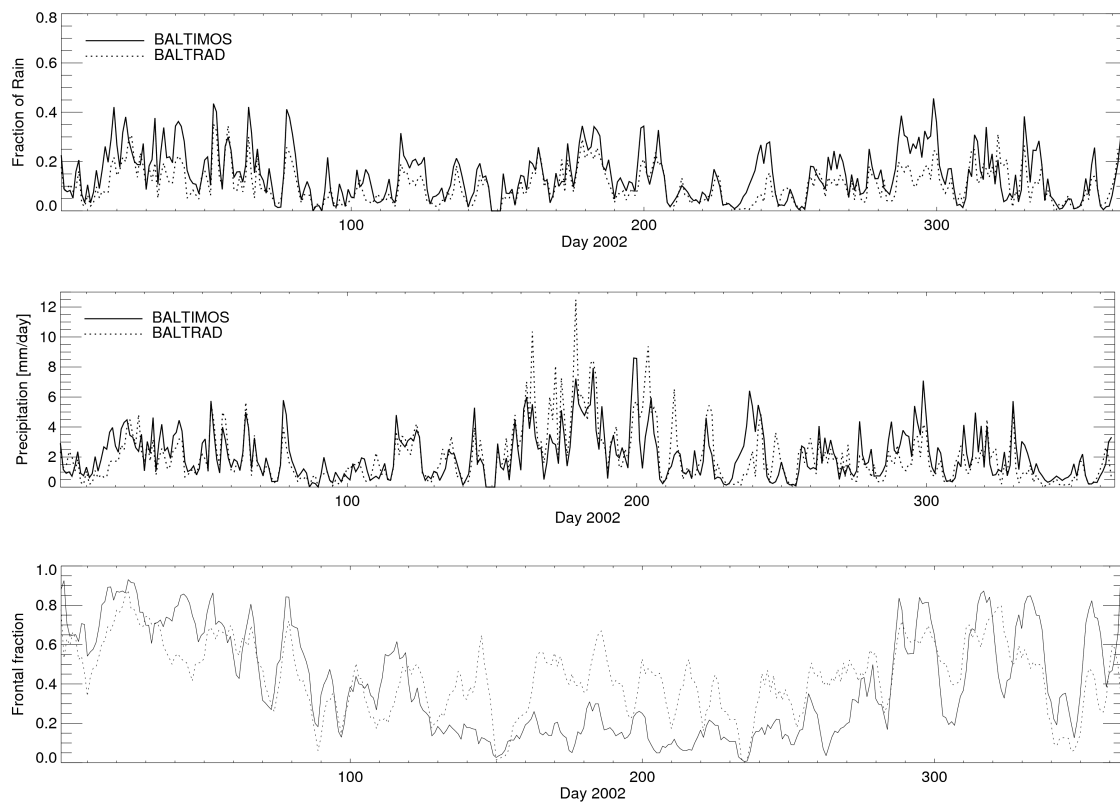


**Figure 6.5:** Same as Fig. 6.3, but for 2002.

Simulation results show only slight differences in the frontal fraction of both surface types as shown in Table 6.2. In contrast, the frontal fraction over land is more than 10 percentage points higher than that over sea in the observations.

### 6.3.3 Diurnal cycle

In this section, simulations of the diurnal variations of rainfall frequency of three years from 2000-2002 are presented, and compared with observations.

Fig. 6.6 maps the spatial distribution of the normalised amplitude  $A_n$  of the first diurnal harmonic of rain events exceeding a threshold of  $0.2 \text{ mmh}^{-1}$  among BALTIMOS and BALTRAD.  $A_n$  is a parameter that describes the ratio between the amplitude of the diurnal cycle and the daily mean (see Eq. 5.3 at Page 39). Thus, this value is dimensionless. For both data sets the amplitude reaches values of about 1, that means the maximal number of rainfall in the diurnal cycle is about twice the daily mean. BALTIMOS map shows a distinctive pattern: Stronger diurnal signals over land and smaller variability above the sea with some exceptions in northern Norway and southern Baltic sea. The coastline is mostly a definite edge of both features. The diurnal cycle in the observations is far less pronounced. The

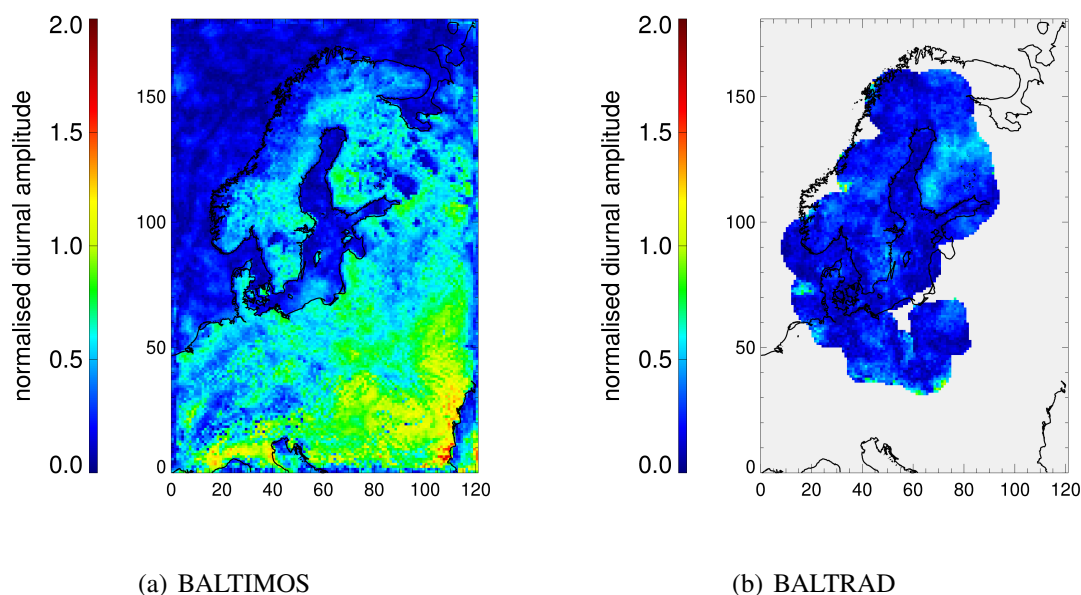


**Figure 6.6:** Simulated and observed spatial patterns of normalised diurnal cycle amplitude of precipitation events. (a) BALTIMOS (b) BALTRAD.

strongest signals appear above Finland with highest values of 1. However, there is no clear land-sea distribution and the values for  $A_n$  are in general lower than in the simulations.

Fig. 6.7 shows the corresponding results by exclusively considering convective events. The diurnal cycle in observations and simulations has a bigger amplitude than at all rain events. The land-sea separation in BALTIMOS is even more distinctive.  $A_n$  reaches values about 1.4 at Baltic Sea area and about 2 for continental precipitation in southern Europe. The amplitude at almost all land surface areas are twice as large the daily mean ( $A_n$  equal 1). Again, the diurnal cycles in observations are weaker. However, with considering only convective events also a definite land-sea discrimination appears, especially at northern Baltic Sea coasts. Coherent areas of regions with high values of  $A_n$  are above Finland with highest values of more than 1.3.

When does the diurnal rainfall cycle peak? Figs. 6.6 and 6.7 show maps of simulated and observed phase of the diurnal cycle. Note that nocturnal peaks are indicated by both, red (before midnight) and blue (after midnight) colour in the phase shift diagrams. Over land, diurnal cycle in BALTIMOS tends to have a maximum at noon for all events with quiet coherent pattern. Convective events have peak hours shifted to afternoon. The behaviour above sea is by far not as coherent. While overall events seem to peak at all hours of day with a weak preference to the late night hours, the trend at convective events is to the hours before midnight. Again, the land-sea separation of diurnal signals with strict edges at the coastline is apparent. The map of peaks for overall events are rather chaotic pattern. That

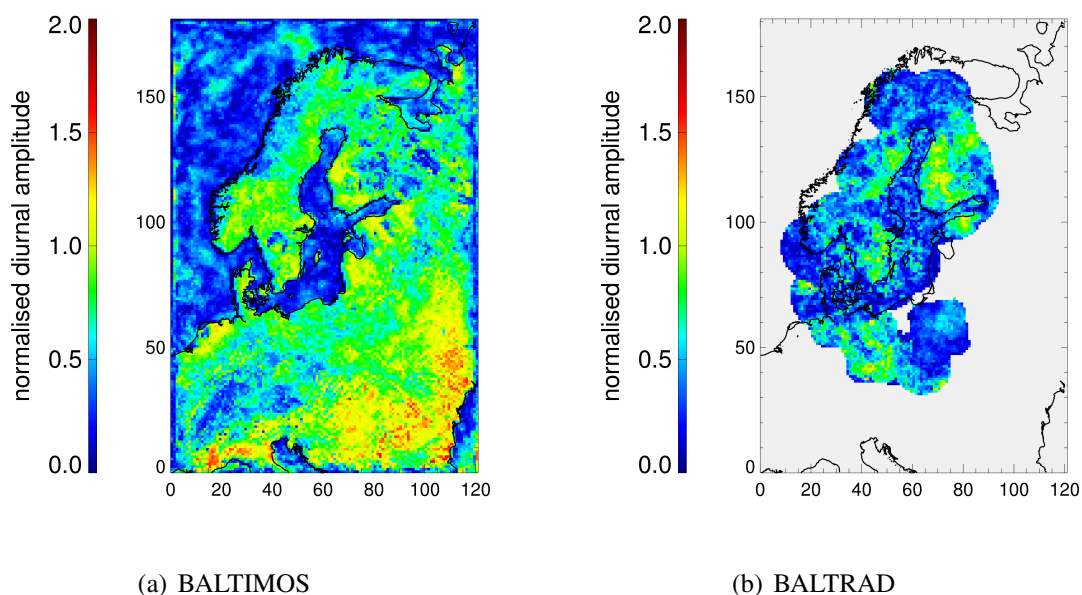


**Figure 6.7:** Same as Fig. 6.6, but for convective events.

is not surprising since weak significance of the diurnal cycle was observed in Fig. 6.6. The diurnal signal for convective events are stronger and therefore the peak map exhibits similar patterns in comparison to simulations: Nocturnal peaks above sea and afternoon peaks above land surface.

To facilitate the discussions, Fig. 6.10 shows the average diurnal cycle of all co-located grid boxes in summer in the Baltic Sea catchment over land (a) and sea (b) separated in overall rain and convective partition. A value of 1 means thereby the daily mean number of precipitation events. Note that the range of the diurnal anomaly is different for both types of surface. Precipitation over land in simulations occurs somewhat earlier as in observations. While BALTIMOS produces a maximum near 1300 LST, the observations peak one to two hours later. This is the case for the overall rainfall and quiet more distinctive for the convective partition. As already shown in the maps the diurnal signals are much stronger for the convective partition. BALTIMOS shows a distinctly greater amplitude with up to twice the normalised daily average. The overall precipitation is featured by less diurnal variations, however, is also characterised by afternoon maxima of precipitation. The left panel of Fig. 6.10 shows that daily precipitation frequency above sea is relatively uniform distributed over the hours of day. The simulations exhibit a peak at afternoon and a secondary early morning peak. It is assumed that the first peak is influenced by land and the latter are the typical nocturnal maxima over sea as described in (Randall et al., 1991).

It might be of particular interest to examine the time shift between the peaks of diurnal cycle for individual grid boxes. Fig. 6.11 maps the time shift between the phase shift of the

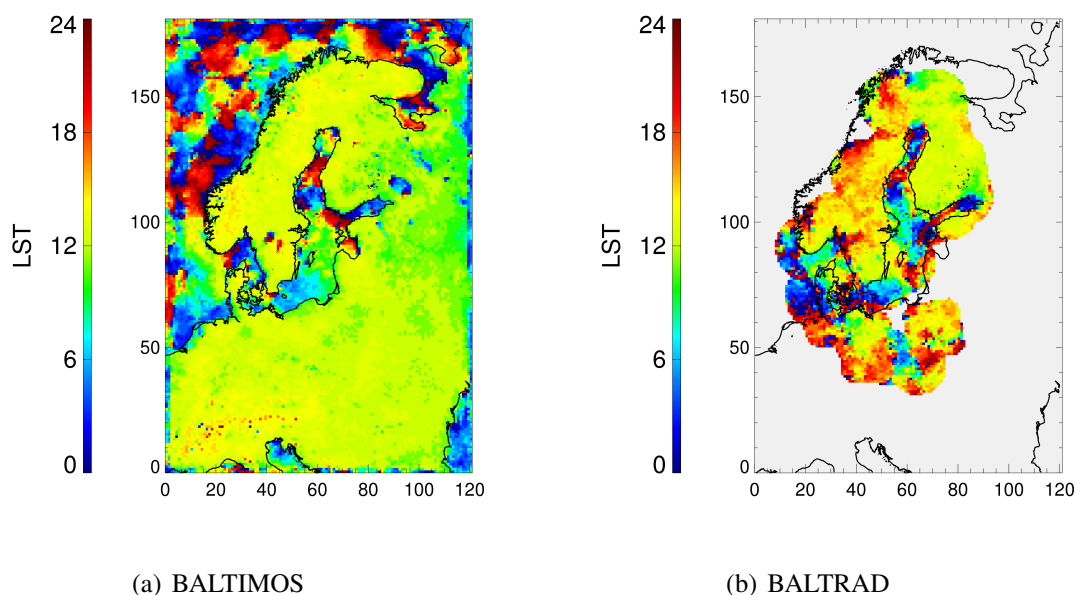


**Figure 6.8:** Simulated and observed spatial patterns of local solar time of maximal value in the diurnal cycle of precipitation events. (a) BALTIMOS (b) BALTRAD.

first harmonic for all grid boxes and for grid boxes with a time shift lower than three hours. Since the diurnal signal over sea is weak large parts of the Baltic Sea exhibits time shifts of more than five hours. It is assumed that the diurnal cycle peaks randomly in these areas. For a better visibility all pixels exceeding the time shift with more than three hours are masked out at the right panel of Fig. 6.11. Red areas indicate that BALTIMOS produces maximal precipitation earlier as the observations. This is the case in large parts of Finland, Sveden and Middle Europe. There are only a few and not contiguous areas where the simulations have peaks shifted to later time in comparison to observations.

Figs. 6.12, 6.13 and 6.14 show sections of normalised amplitude of the first convective rain harmonic along three west-east lines within the Baltic sea. Sea regions are shaded blue. The associated local hour of the peak in the diurnal convective rainfall cycle for every full longitude degree is shown as clock arrow signs above the image. The main features of land and sea regions are well cognisable in all three sections: Higher amplitude with afternoon peaks over land and weak diurnal variability with nocturnal or random peaks above the sea. This was already discussed before in connexion to Figs. 6.6 to 6.10. The interesting thing in the figures here are the behaviour directly at the coastlines. While BALTIMOS has a very strict differentiation between land and sea characteristics with an abrupt decrease of the diurnal signal if coming from land to sea, the decrease in the observations is far weaker and smoother (e.g. very typically at longitude  $19^\circ$  in Fig. 6.12) The observations still exhibit some afternoon peaks over sea.

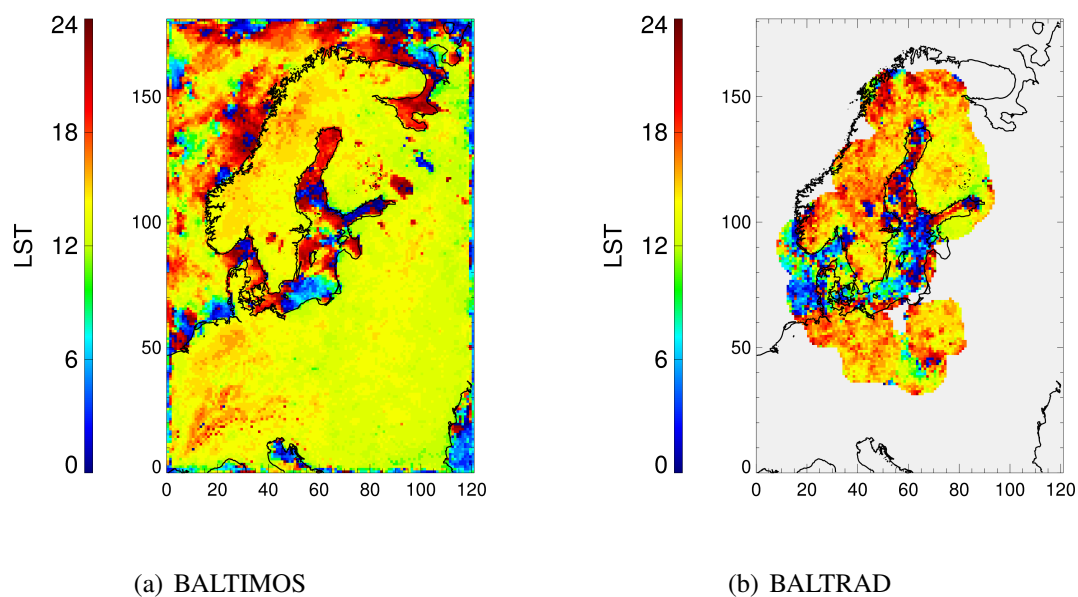


**Figure 6.9:** Same as Fig. 6.8, but for convective events.

To express a broad generalisation, there are two typical types of diurnal cycles: a land type with large variability and afternoon peaks and a sea type with only weak variability and a tendency to nocturnal peaks. This approach are increased observable with convective precipitation. In relation to this, Figs. 6.6 to 6.9 exhibit a feature worthwhile to investigate more thoroughly. While the observations show blurred overlaps of the boundary between both types of diurnal behaviour and the coastlines, BALTIMOS produces a rather accurate overlap. Figs. 6.12, 6.13 and 6.14 show sections of the normalised amplitude along three different rows of BALTIMOS grid. In order to make the land-sea behaviour more visible sea pixels are shaded blue. The phase shift is shown as a clock sign for every 5th pixel without any interpolation above the diagrams. The most southern section (Fig. 6.12) exhibits very clearly this feature: There is an abrupt decrease of amplitude at the coast in simulations and a far smoother decrease in observations. Peaking hours are not clearly coherent above sea, however there are more nocturnal and early morning peaks in simulations than in observations. Observations tend to peak at evening hours above sea.

## 6.4 Conclusions

The purpose of this section is to examine precipitation output in BALTIMOS with a special focus on diurnal variability and the frontal/convective classification in the Baltic area. This section summaries the results of the analysis. Observational data and simulations of the regional climate system BALTIMOS are used to study several aspects of precipitation in

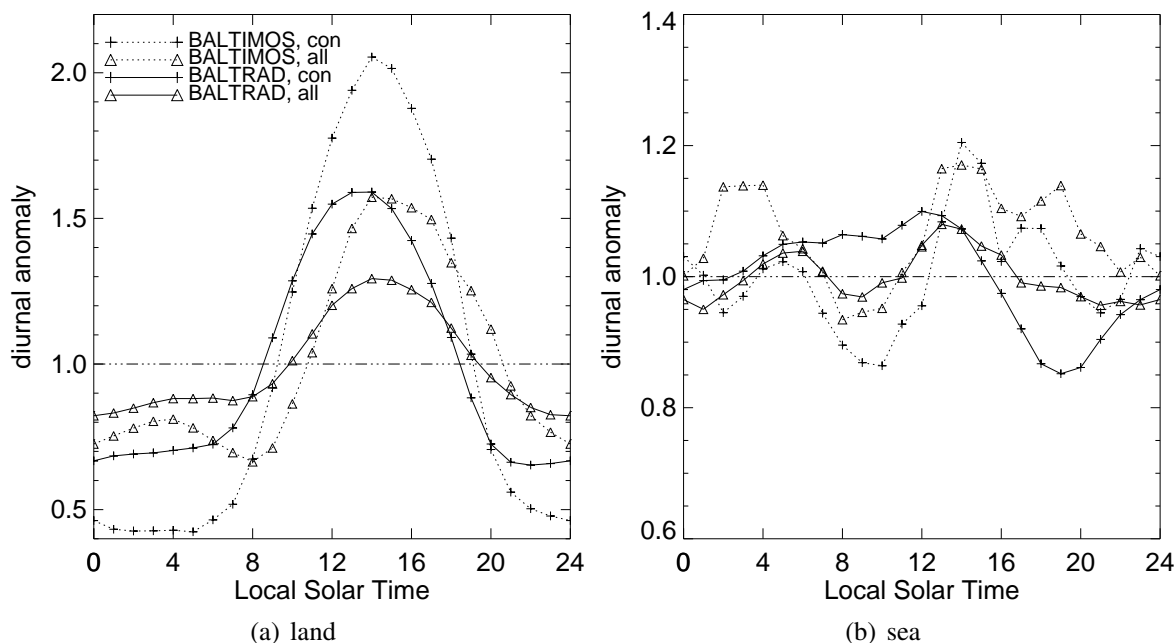


**Figure 6.10:** Mean diurnal variations of BALTIMOS (solid curves) and BALTRAD (dashed curves) precipitation for summer in 2000-2002 for all events (triangle symbol) and convective events (cross): a) land pixels, b) sea pixels.

the Baltic sea and its drainage basin with a special focus on the diurnal cycle. The study includes a general evaluation of precipitation, showing that BALTIMOS has too many light rain events causing an overestimation of the total annual amount. The diurnal cycle as well as its spatial distribution were analysed. BALTIMOS captures the broad characteristics: Significant diurnal variability with an afternoon peak above land and weak variability with a nocturnal peak above sea. An algorithm to distinguish between frontal and convective precipitation is applied to examine the diurnal cycle more thoroughly. Comparing with the radar measurements the time of maximum convective rain in summer is about one to two hours shifted to the time with largest surface heating in the simulations.

By comparing the precipitation data between BALTIMOS and GPCC gauge data, the model captures the general patterns, but overestimates the yearly sums up to a third. Rain with very low rain rate (less than  $0.1 \text{ mmhr}^{-1}$ ) provide a substantial portion to the total amount in BALTIMOS. However, the actual situation in the atmosphere is not clear, because estimation of the amount of drizzle by radar and rain gauges remains difficult. The simulations of the frontal fraction is in a good agreement with the observations if one only consider the yearly values. The classification results differ according to the occurrence of long periods with frontal overpasses significantly. Comparisons of simulations and observations on diurnal characterisations indicate that the model triggers convective precipitation too early at the hour of the day. Rain in BALTIMOS falls mainly shifted to midday. The assumption is,



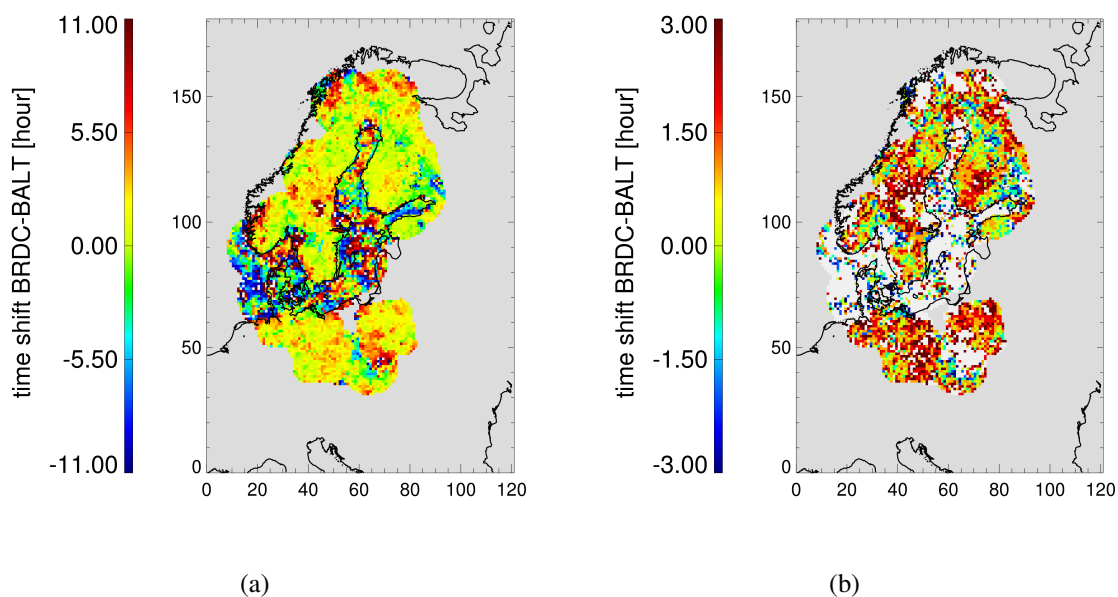


**Figure 6.11:** Time shift between hours of peak in the diurnal cycle of observations and simulations (BALTRAD-BALTIMOS). (a) all pixels. (b) only pixels with a time shift lower than 3 hours.

that summer convection has less time to accumulate precipitable water within clouds. That is eventually resulting in the absence of heavy rain intensities. Another consequence appears in the spatial distribution. Figs. 6.6 and 6.9 exhibit a strict land-sea differentiation in respect to the amplitude of the diurnal rain curve as well as the hour of peaking in BALTIMOS. On the other hand, the observations show a blurred edge of pixels with sea or land characterisations. That indicates, that typical sea and land behaviour of diurnal cycle is in any kind "advected" in observations, but not in the model. That conclusion for that finding is that convective rain in the model precipitate too early and does not being transported horizontally. It tends to fall at the place where the convective lifting of air occurs.

It could be proven, that the separation in frontal and convective partition are a valuable tool for the evaluation of climate models.

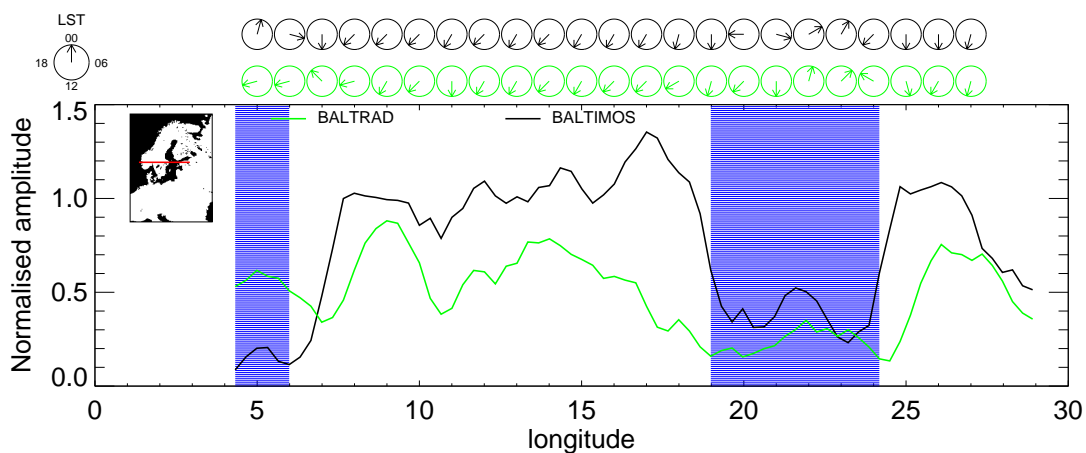


**Figure 6.12:** First diurnal harmonic of precipitation events: Section of normalised amplitude along indicated line seen in the inset (row nr.100 of BALTIMOS grid). Blue shaded regions are sea surface regions. Clock arrows above the diagram pointing upward indicate maxima at local midnight (00:00 LST), those pointing to the right indicate maxima 06:00 LST, etc. Note that clock arrows are shown for every 5th grid box (column 5,10, etc.) and are not interpolated values.

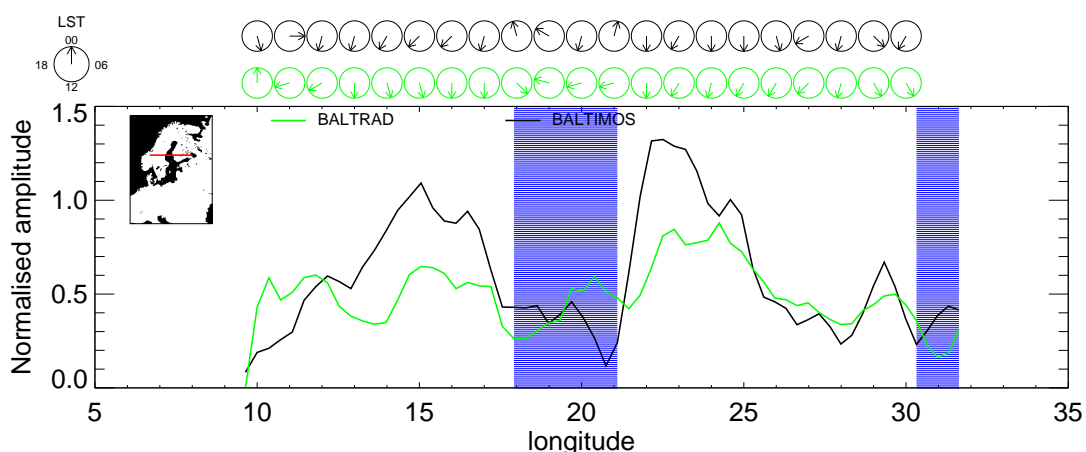


**Figure 6.13:** Same as Fig. 6.12, but for row nr.115 as shown in the inset.

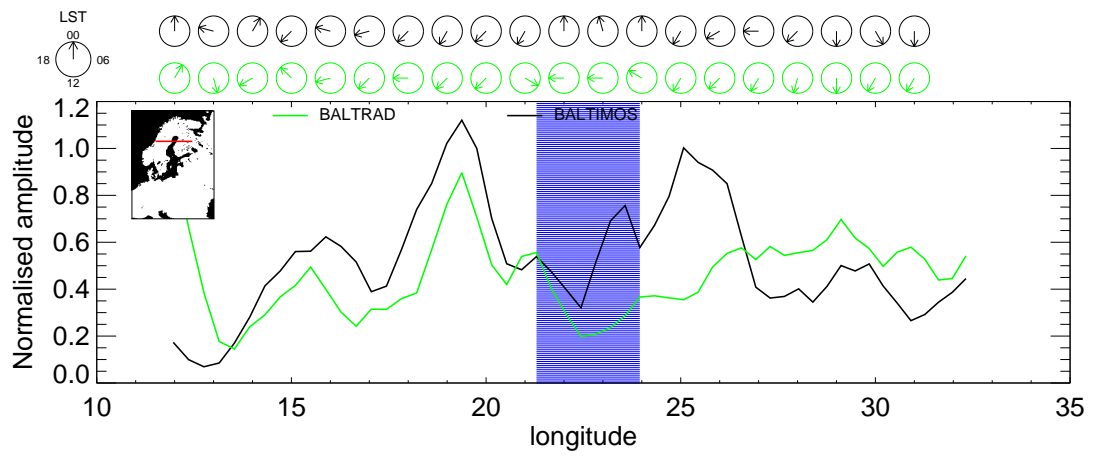


**Figure 6.14:** Same as Fig. 6.12, but for row nr.130 as shown in the inset.

